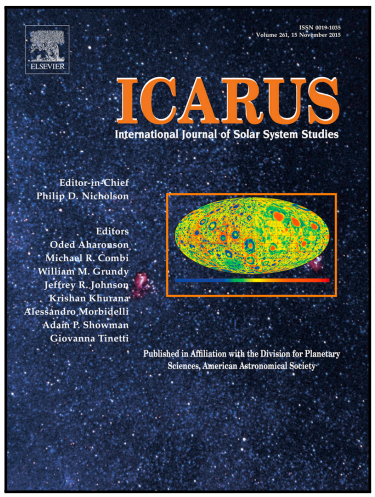

The Mineralogy of Ceres' Nawish Quadrangle

F.G. Carrozzo , F. Zambon , M.C. De Sanctis , A. Longobardo , A. Raponi , K. Stephan , A. Frigeri , Ammannito , M. Ciarniello , J.-Ph. Combe , E. Palomba , F. Tosi , C.A. Raymond , C.T. Russell

PII: S0019-1035(17)30330-5
DOI: 10.1016/j.icarus.2018.07.013
Reference: YICAR 12962

To appear in: *Icarus*

Received date: 29 April 2017
Revised date: 19 June 2018
Accepted date: 13 July 2018

Please cite this article as: F.G. Carrozzo , F. Zambon , M.C. De Sanctis , A. Longobardo , A. Raponi , K. Stephan , A. Frigeri , Ammannito , M. Ciarniello , J.-Ph. Combe , E. Palomba , F. Tosi , C.A. Raymond , C.T. Russell , The Mineralogy of Ceres' Nawish Quadrangle, *Icarus* (2018), doi: 10.1016/j.icarus.2018.07.013

HIGHLIGHTS

- Sodium carbonates are found in bright material in ejecta craters
- Mineralogy of quadrangle Nawish using the band at 2.7, 3.1 and 3.9 µm.
- Correlation between age of terrains and the mineralogy

The Mineralogy of Ceres' Nawish Quadrangle

F.G. Carrozzo[1], F. Zambon[1], M.C. De Sanctis[1], A. Longobardo[1], A. Raponi[1], K. Stephan[2], A. Frigeri[1], Ammannito[1,3], M. Ciarniello[1], J.-Ph. Combe[4], E. Palomba[1], F. Tosi[1], C.A. Raymond[5], C.T. Russell[6]

1. Istituto di Astrofisica e Planetologia Spaziali, INAF, Via del Fosso del Cavaliere 100, 00133 Roma, Italy

2. DLR, Institute of Planetary Research, Berlin, Germany

3. Agenzia Spaziale Italiana, ASI, via del Politecnico, 00133 Roma, Italy

4. Bear Fight Institute, Winthrop, WA, USA

5. Jet Propulsion Laboratory, California Institute of Technology, Pasadena, CA, USA

6. Earth Planetary and Space Sciences, University of California, Los Angeles, CA, USA

Abstract

Quadrangle Ac-H-08 Nawish is located in the equatorial region of Ceres (Lat 22°S-22°N, Lon 144°E-216°E), and it has variable mineralogy and geology. Here, we report on the mineralogy using spectra from the Visible and InfraRed (VIR) mapping spectrometer onboard the NASA Dawn mission. This quadrangle has two generally different regions: the cratered highlands of the central and eastern sector, and the eastern lowlands. We find this dichotomy is also associated with differences in the NH_4-phyllosilicates distribution. The highlands, in the eastern part of the quadrangle, appear depleted in NH_4-phyllosilicates, conversely to the lowlands, in the north-western side. The Mg-phyllosilicates distribution is quite homogeneous across Nawish quadrangle, except for few areas. The 2.7-μm band depth is lower in the south-eastern part, e.g. in the Azacca ejecta and Consus crater ejecta, and the band depth is greatest for the Nawish crater ejecta, and indicates the highest content of Mg-phyllosilicates of the entire quadrangle. Our analysis finds an interesting relationship between geology, mineralogy,

topography, and the age in this quadrangle. The cratered terrains in the highlands, poor in NH_4 phyllosilicates, are older (~2 Ga). Conversely, the smooth terrain, such as with Vindimia Planitia, is richer in ammonia-bearing phyllosilicates and is younger (~1 Ga). At the local scale, Ac-H-8 Nawish, displays several interesting mineralogical features, such as at Nawish crater, Consus crater, Dantu and Azzacca ejecta, which exhibit localized Na-carbonates deposits. This material is superimposed on the cratered terrains and smooth terrains and shows the typical depletion of phyllosilicates, already observed on Ceres in the presence of Na-carbonates.

1. Introduction

Dwarf planet Ceres, the first and most massive discovered in the main-asteroid belt, is a unique remnant of the primordial population of large planetesimals (Morbidelli et al., 2009; Perna et al., 2015). Unlike Vesta and other bodies of the Solar System, Ceres is not associated with any clan of meteorites. Its surface is quite dark (albedo 0.10 ± 0.01, Tedesco et al., 1983), and resembles carbonaceous chondrites (CM, Johnson and Fanale 1973; Larson et al. 1979; McSween et al., 2017; see McCord and Castillo-Rogez, 2018 for a review).

After the earliest spectral exploration of Ceres' surface composition suggesting aqueous alteration, ground based observations indicated more specific mineralogies: H_2O/OH (Lebofsky, 1978), suggesting the presence of a layer of water ice frost (Lebofsky et al., 1981), ammoniated phyllosilicates (King et al., 1992), a mixture of crystalline water ice and organic component (Vernazza et al., 2005), a mixture of iron-rich clay and carbonates (Rivkin et al., 2006), a mixture of carbonates and brucite (Milliken and Rivkin, 2009), or goethite and carbonates (Beck et al., 2011).

In 2015, Dawn spacecraft entered orbit around Ceres (Russell and Raymond, 2011; Russell et al., 2016), confirming most previous studies and unveiling unknown aspect of the dwarf planet' surface. Ceres average spectrum acquired by Visible and InfraRed spectrometer (VIR, De Sanctis et al., 2011) onboard Dawn, shows several absorption bands in the spectral domain between 1 and 5 μm (De Sanctis et al., 2015). These spectral signatures are located at 2.72–2.73 μm, 3.05–3.10 μm, 3.3–3.4 μm, and 3.95-4.02 μm. The prominent 2.72–2.73 μm band is diagnostic of hydrous minerals, more specifically Mg-phyllosilicates, the 3.05–3.1 μm band is associated with NH_4-phyllosilicates, and the 3.3-3.4 μm band, which may be typical of organic compounds (Clark, 1999; De Sanctis et al., 2017a), can also be diagnostic of carbonates when observed in conjunction with the ~4 μm band (Milliken and Rivkin, 2009). Hereafter, for simplicity we will refer to the band centered at 2.72 μm as the 2.7 μm band, the band centered at 3.05–3.1 μm as the 3.1 μm band, the band centered at 3.3–3.5 μm as the 3.4 μm band, and the band centered at 3.95-4.02 μm as the 4 μm band.

Ceres' surface has been divided into 15-tile quadrangles, commonly used for medium-sized planetary bodies (Greeley and Batson, 1990). Each quadrangle was named following the nomenclature indicated in Roatsch et al., 2016. In this paper, we describe the mineralogy of the Ac-H-8 Nawish quadrangle, covering a portion of the equatorial region of Ceres (lon 144°E-216°E, lat 22°S-22°N). The 80-km Nawish crater (centered at 194.2°E and 12.2°N), located in the northern region, namesakes the quadrangle.

2. Dataset and Methods

In about 3 years orbiting around Ceres, Dawn acquired data at different spatial resolution, based on the altitude of the spacecraft from the surface. The spectral maps shown in this paper were obtained by

VIR at spatial resolution of ~380 m/pixel, during the High Altitude Mapping Orbit (HAMO) mission phase. The data have been calibrated following the procedure described by Filacchione and Ammannito (2014). Afterwards, (i) we removed the instrumental artifacts from the calibrated data (Carrozzo et al., 2016); (ii) we removed the thermal emission from the spectra (Raponi et al. 2017, this issue); (iii) then we applied a photometric correction based on the Hapke model (Ciarniello et al., 2017); (iv) finally, we computed and produced proper spectral parameters maps, as described by Frigeri et al., 2018a (this issue). To complement our analysis, we included also some relevant maps derived by Framing Camera (FC; Sierks et al., 2011) data. FC data have been calibrated following the method described in Schröder et al. (2013) and has a spatial resolution ~2.67 times better than VIR (Sierks et al., 2011). FC is equipped with 7 narrow-band filters centered at different wavelengths in the overall spectral range ~0.4–1.0 μm for compositional analysis, and a broad band clear filter devoted to geologic analysis (Sierks et al., 2011). In all maps, longitudes are East oriented, and are given in the Ceres coordinate system (Roatsch et al., 2016).

3. Tools and techniques

To carry out our analysis, we used the most useful spectral parameters derived from the VIR spectra, i.e. those showing the larger variability, considering also the support of some FC maps.

3.1. Framing camera maps

FC data provide a high-resolution context that is useful to complement our mineralogical analysis of Ceres. We considered some FC derived mosaics: a reflectance mosaic obtained in the clear filter (map scale ~140 m/pixel) (Fig. 1), a RGB composite mosaic: R: F5/F3 (965 nm/749 nm), G: F2/F3 (555

nm/749 nm), and B: F8/F3 (438 nm/749 nm) (Fig. 2), a portion of the digital terrain model at a scale of 60 meter/pixel (Fig. 3), and finally a geologic map that allows us to associate geologic and mineralogical units (Fig. 4). Nawish quadrangle topography is computed as the height over an ellipsoid with a semi-major axis of 482 km and a semi-minor axis of 446 km, showing an elevation ranging between -3800 m and 5900 m (Frigeri et al., 2018b).

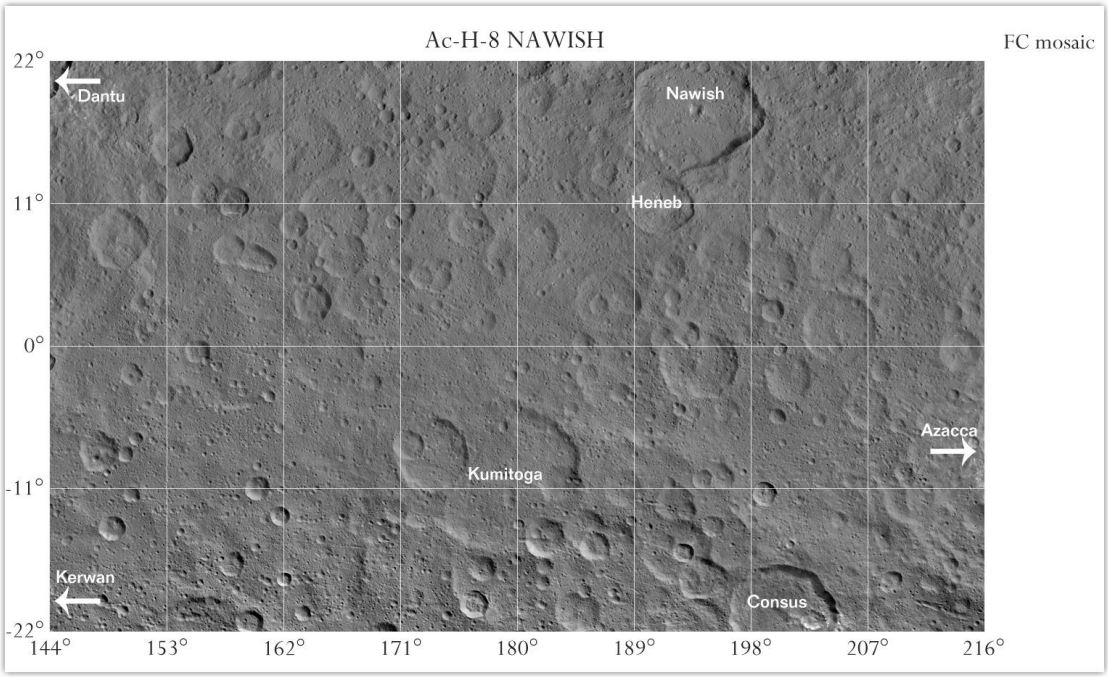

Figure 1. Reflectance map of Ac-H-8 Nawish, obtained through photometric correction of FC clear-filter data acquired in the HAMO mission phase. The map scale is ~140 m/pixel.

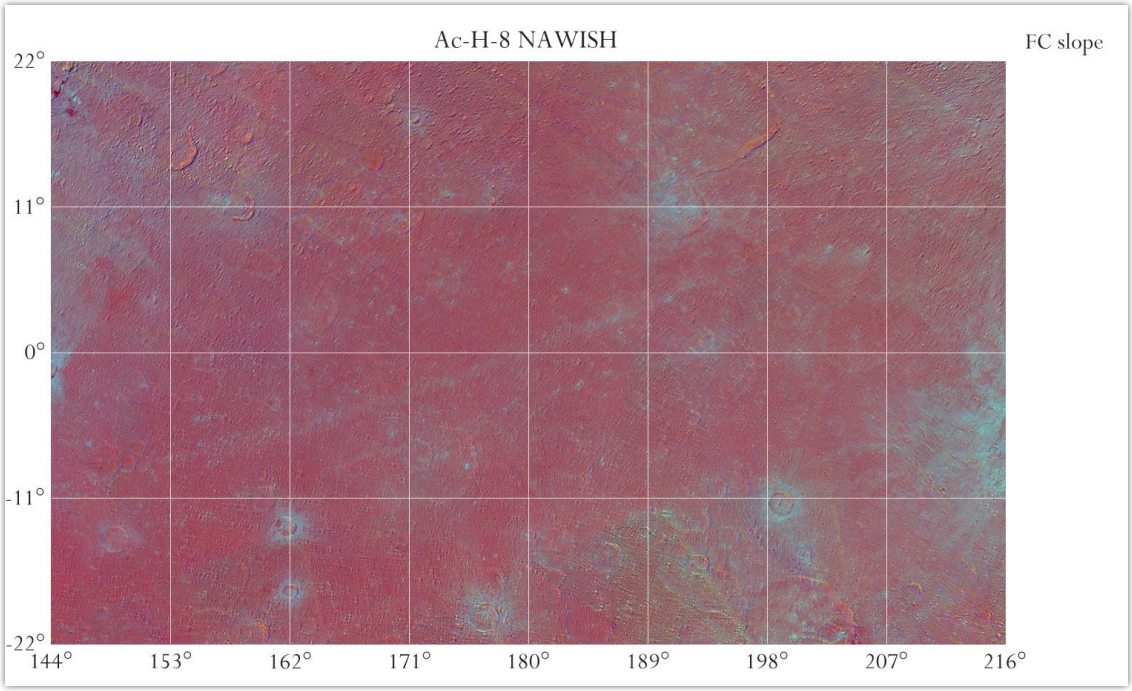

Figure 2. RGB composite map of the Ac-H-8 Nawish quadrangle made from FC color ratios: F5/F3 (965 nm/749 nm), F2/F3 (555 nm/749 nm), and F8/F3 (438 nm/749 nm). Color ratios may enhance differences in material and composition.

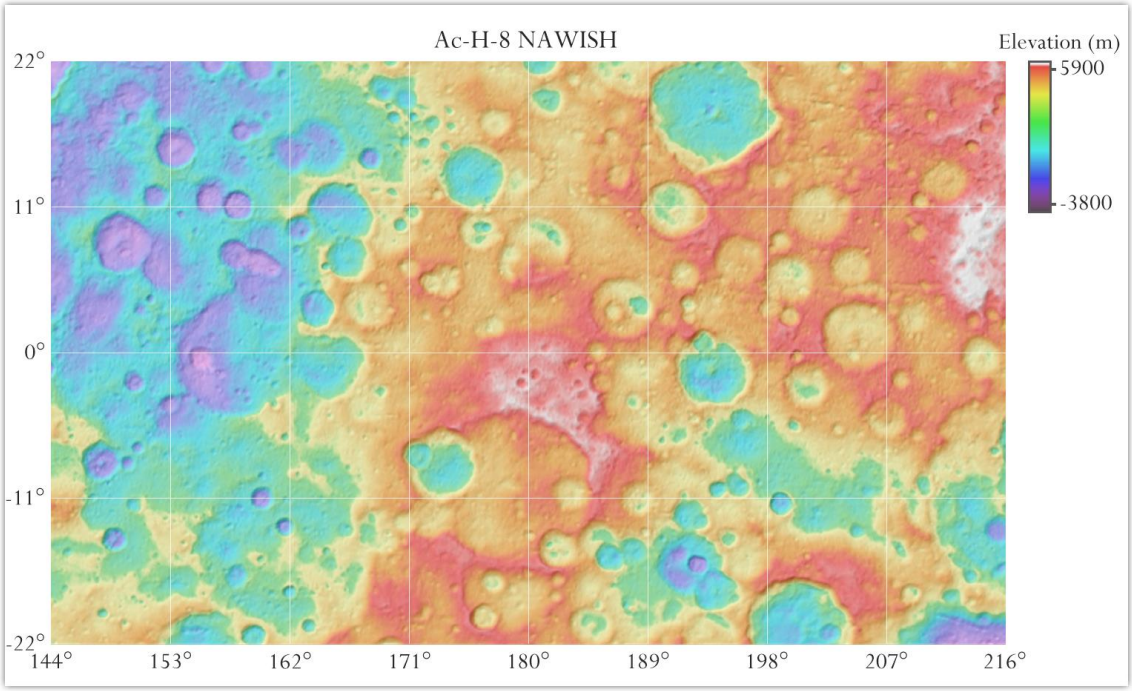

Figure 3. Portion of the digital terrain model (DTM) derived from FC images acquired in HAMO mission phase (Preusker et al., 2016). The color palette follows height in m with respect to the reference ellipsoid (i.e., the curvature of the body is removed), with the highest elevations in red and the lowest terrains in blue.

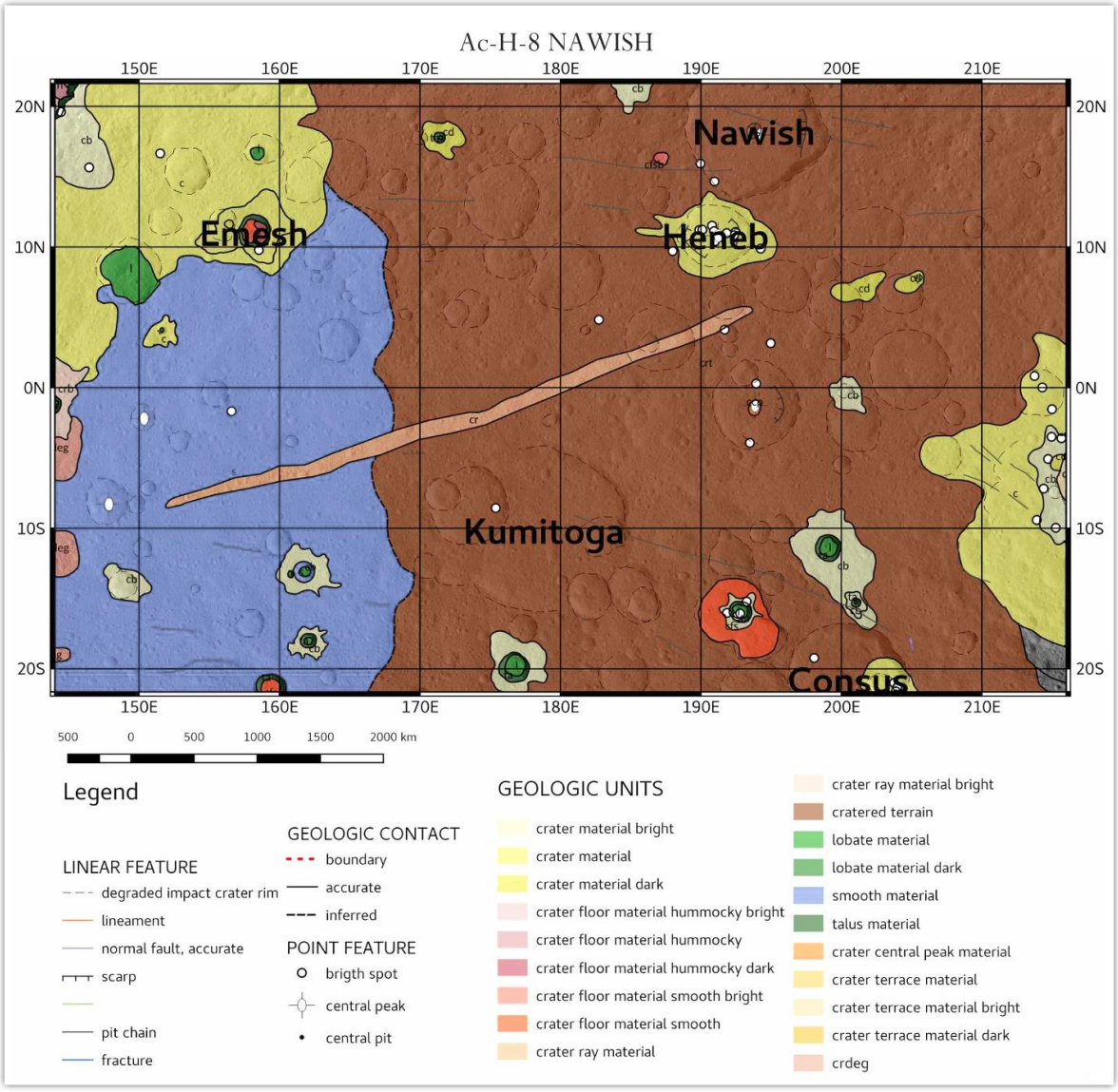

Figure 4. Geological map of Ac-H-8 Nawish quadrangle, from Frigeri et al. (2018b). The broad brownish geologic unit is mapped as ‘cratered terrain’ (crt). Yellow patches represent ‘crater material’, (c) while blue unit indicates ‘smooth material’ (sm).

3.2. VIR maps

Reflectance spectra acquired by the VIR spectrometer are representative of Ceres' uppermost soil layer. Spectral parameters have been used successfully in the past for different bodies of the Solar System (e.g., Pelkey et al., 2007; Carrozzo et al., 2012). To study the mineralogy of Ceres, maps of the main spectral parameters have been produced. Below, we report a brief description of the spectral indices considered in this special issue (for more details see Frigeri et al., 2018a, this issue).

3.2.1. Albedo maps at 1.2 μm

Albedo maps refer to VIR data at 1.2 μm (Fig. 5). We selected this wavelength to avoid spectral regions known or expected to host diagnostic signatures, and it is therefore optimal to sample the spectral continuum. This parameter can be related to the grain size and composition. Previous studies (e.g. Carrozzo et al., 2018) showed that occurrence of carbonate content increases the reflectance while the opaque causes darkening. Albedo was calculated by applying a Hapke photometric correction to the entire dataset as described by Ciarniello et al., 2017.

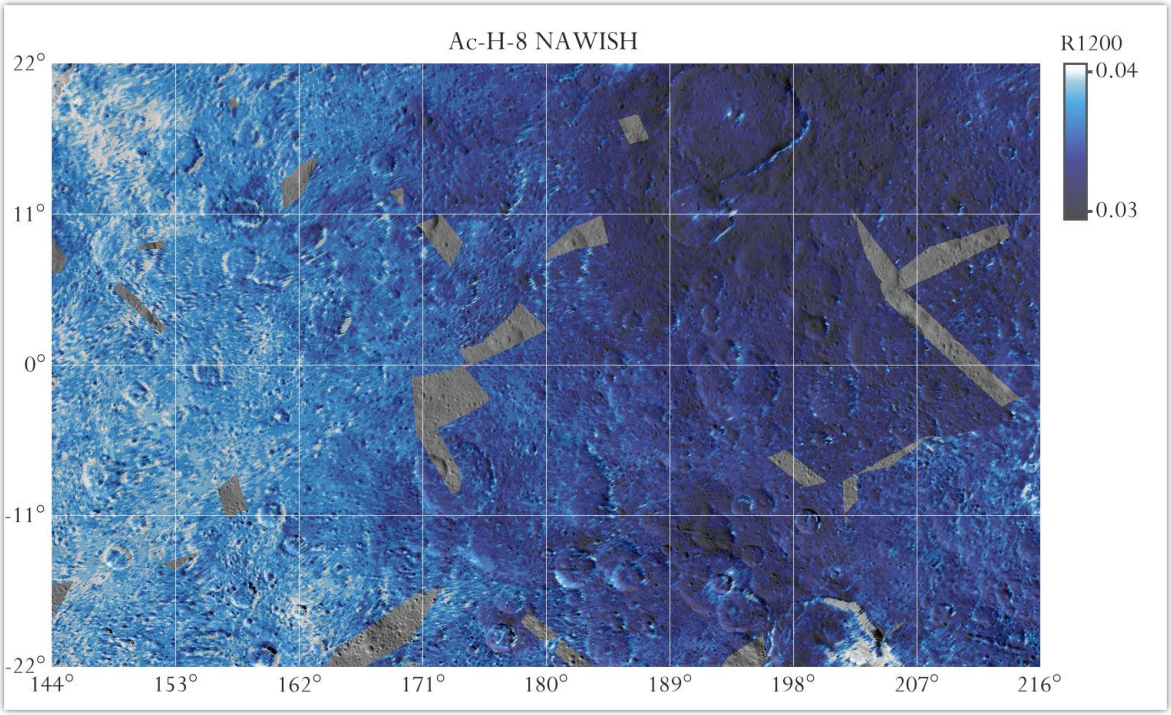

Figure 5. Reflectance map of Ac-H-8 Nawish, obtained through photometric correction of VIR data acquired at 1.2 μm in the HAMO mission phase, interpolated on a grid with a fixed resolution of 140 m/pixel, photometrically corrected by using the method described by Ciarniello et al. (2017), i.e. a Hapke photometric correction to standard observation geometry (i = 30°, e = 0°, α = 30°). The map is superimposed over the Framing Camera (FC) images using a transparence of 25%.

3.2.2. Infrared spectral slope

The spectral slope (Fig. 6) is a useful parameter to investigate surface properties. We computed the spectral slope map in the infrared domain where no absorption features show up. In particular, we selected the spectral slopes between 1.163–1.891 μm (hereafter ISS). To calculate the spectral slope we used the method described in Cuzzi et al. (2009) and Filacchione et al. (2012). Details concerning the production of such maps are reported in Frigeri et al. (2018a, this issue).

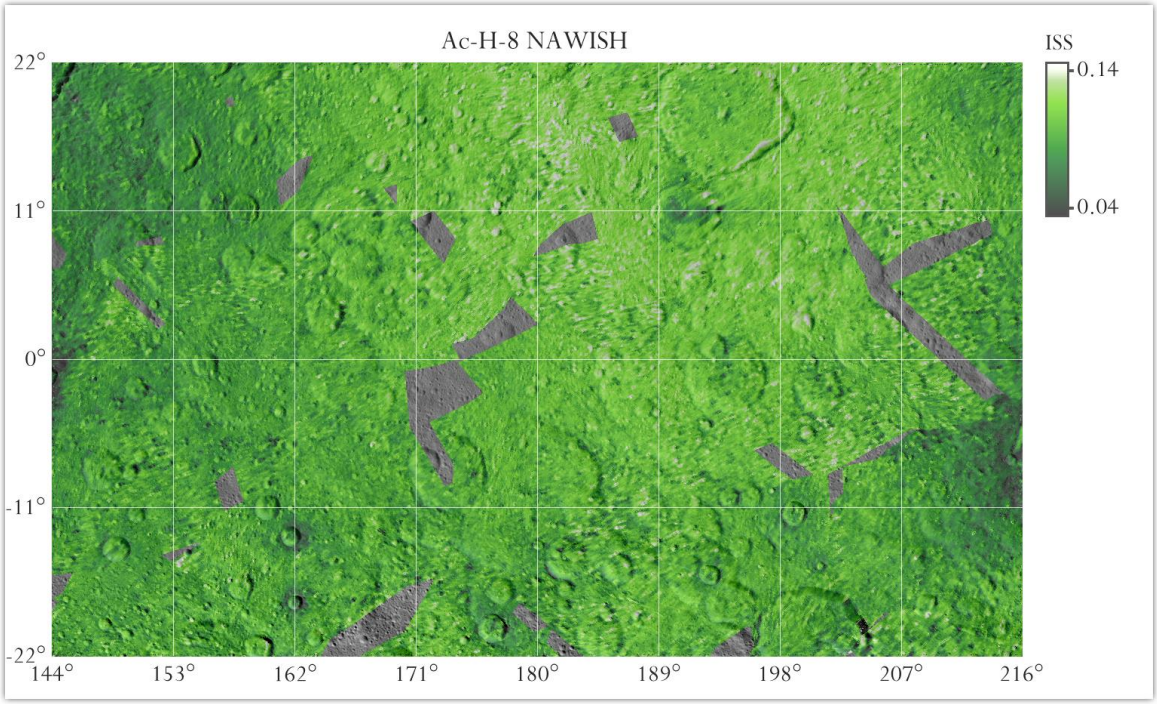

Figure 6: VIR spectral slopes calculated in the near infrared range 1.163–1.891 μm (ISS). The map is superimposed over the FC images using a transparence of 25%.

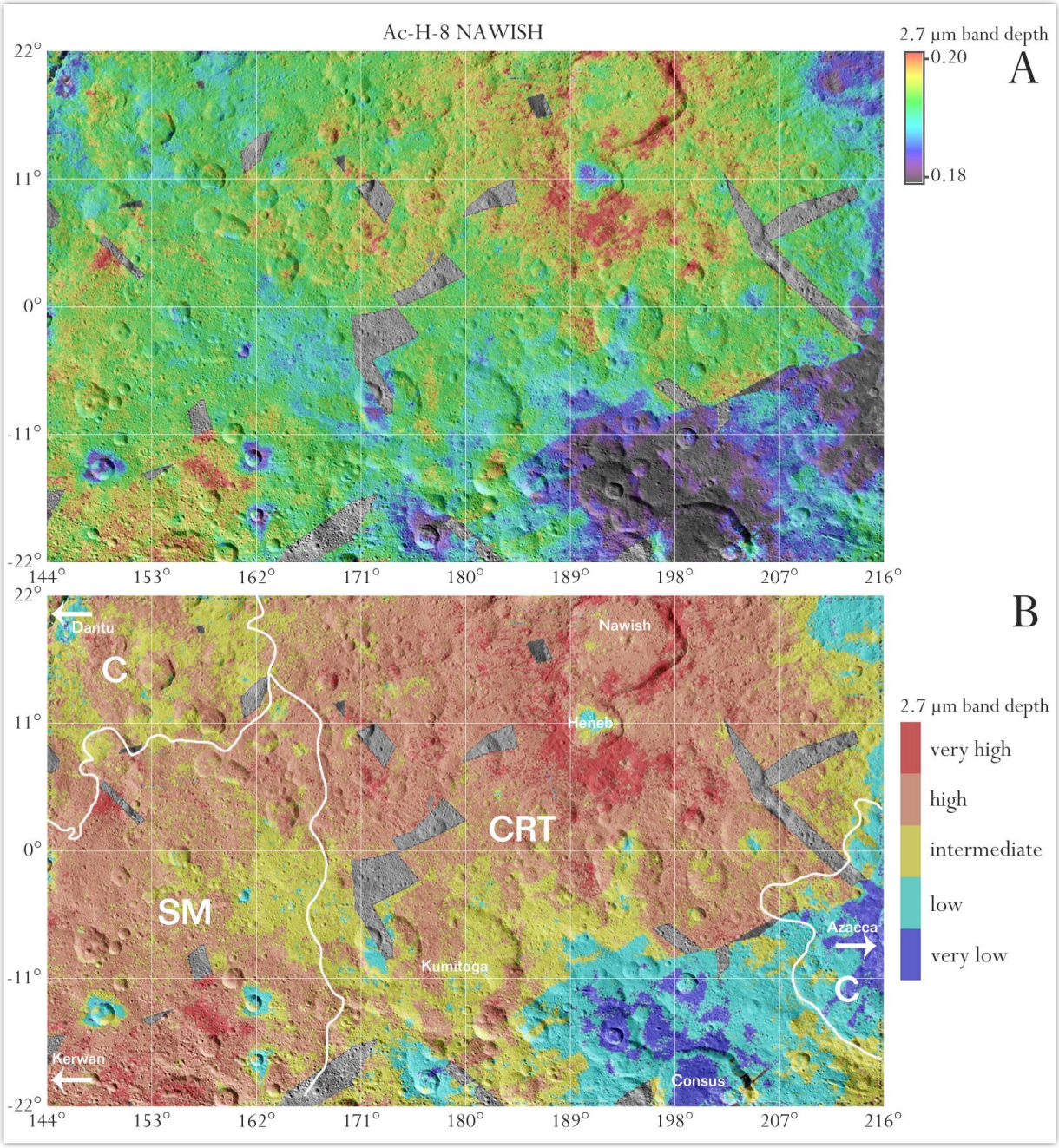

Figure 7. (A) 2.7 µm band depth VIR-derived map of the Nawish quadrangle. (B) The map shown in Panel A divided in 5 different ranges of values to emphasize its relationship with the geological units. The boundary of some geological units has been drawn (white curves: CRT = cratered terrains, C = crater material, SM = smoothed material, for details see Frigeri et al., 2018b). The map is superimposed over the FC images using a transparence of 25%.

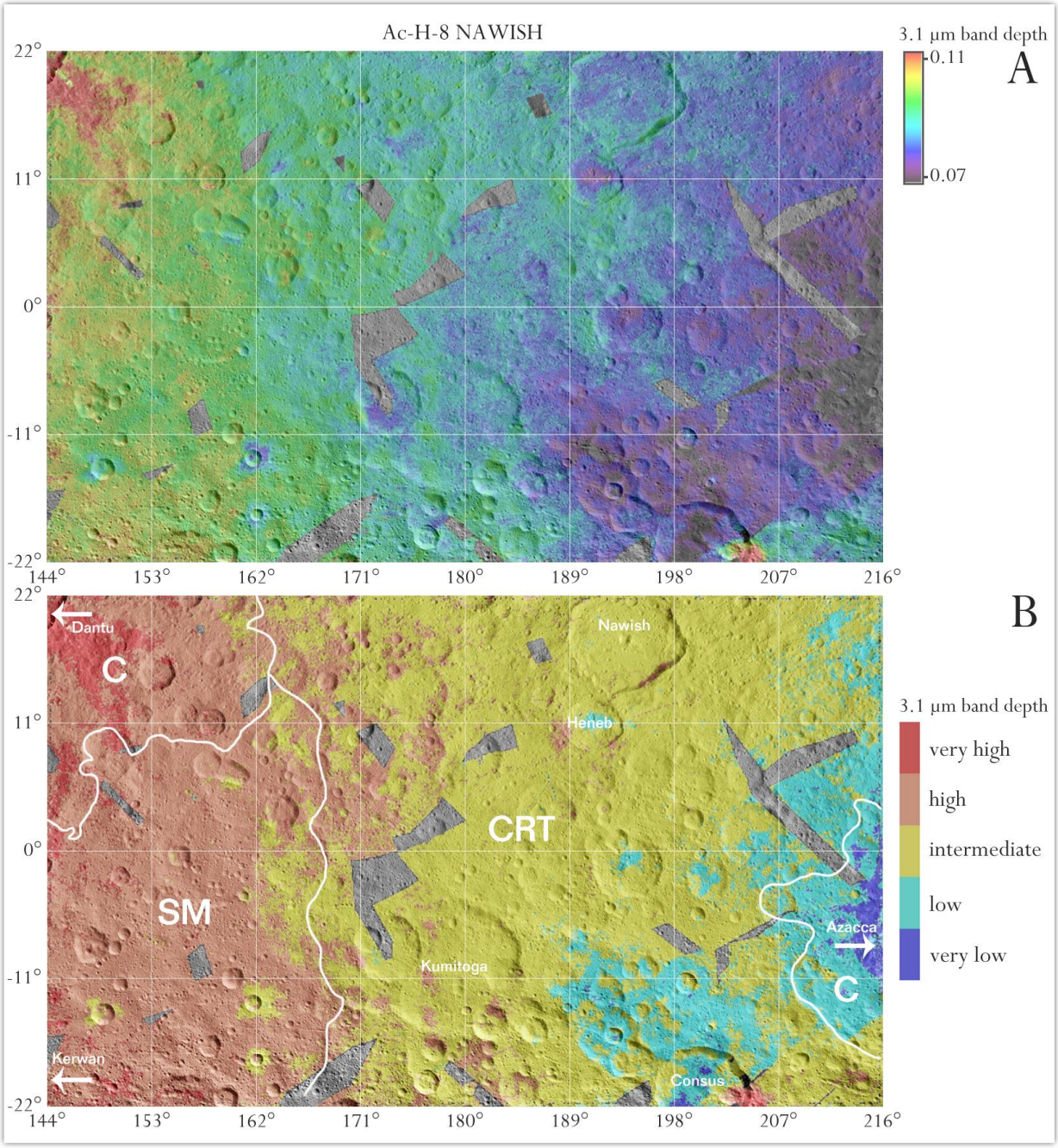

Figure 8. (A) 3.1 µm band depth VIR-derived map of the Nawish quadrangle. (B) The map shown in Panel A divided in 5 different ranges of values to emphasize its relationship with the geological units. The boundary of some geological units has been drawn (white curves: CRT = cratered terrains, C = crater material, SM = smoothed material, for details see Frigeri et al., 2018b). The map is superimposed over the FC images using a transparence of 25%.

3.2.3. Band depths at 2.7 and 3.1 μm

The average reflectance spectrum of Ceres displays a set of absorption bands (De Sanctis et al., 2015). Here we map the band depths at ~2.7 (Fig. 7) and ~3.1 μm (Fig. 8). They are associated with Mg-phyllosilicates and NH_4-phyllosilicates, respectively (De Sanctis et al., 2015), and are ubiquitous at the spatial resolution of 1.1 km/pixel (Ammannito et al., 2016). The depth of a band gives information about the abundance of the absorbing minerals, but it could be also affected by the presence of opaque materials and by the grain size (Clark, 1999). For a detailed description, we refer to Frigeri et al. (2018a, this issue).

3.2.4. Band center and band depth 4 μm

The 4 μm absorption band, indicative of carbonates, is also ubiquitous on Ceres. Fig. 9 shows the band center and depth distribution of this signature across the Nawish quadrangle. To produce the maps of this band we used the same method for the 2.7 and 3.1 μm bands computation (for detail see Carrozzo et al., 2018).

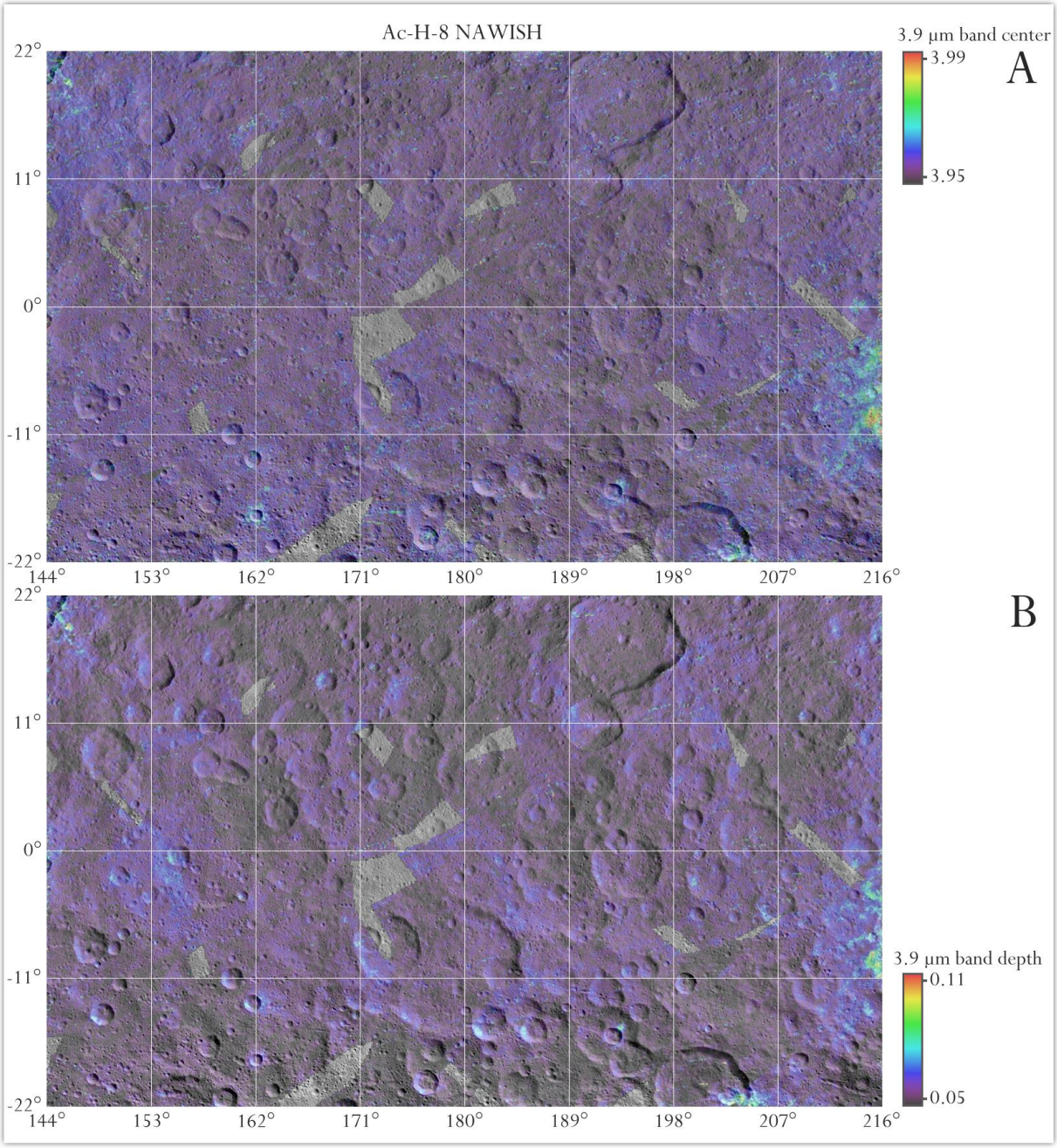

Figure 9. A) band center and B) band depth at 4 μm VIR-derived map of the Ac-H-8 Nawish quadrangle. The map is superimposed over the FC images using a transparence of 25%.

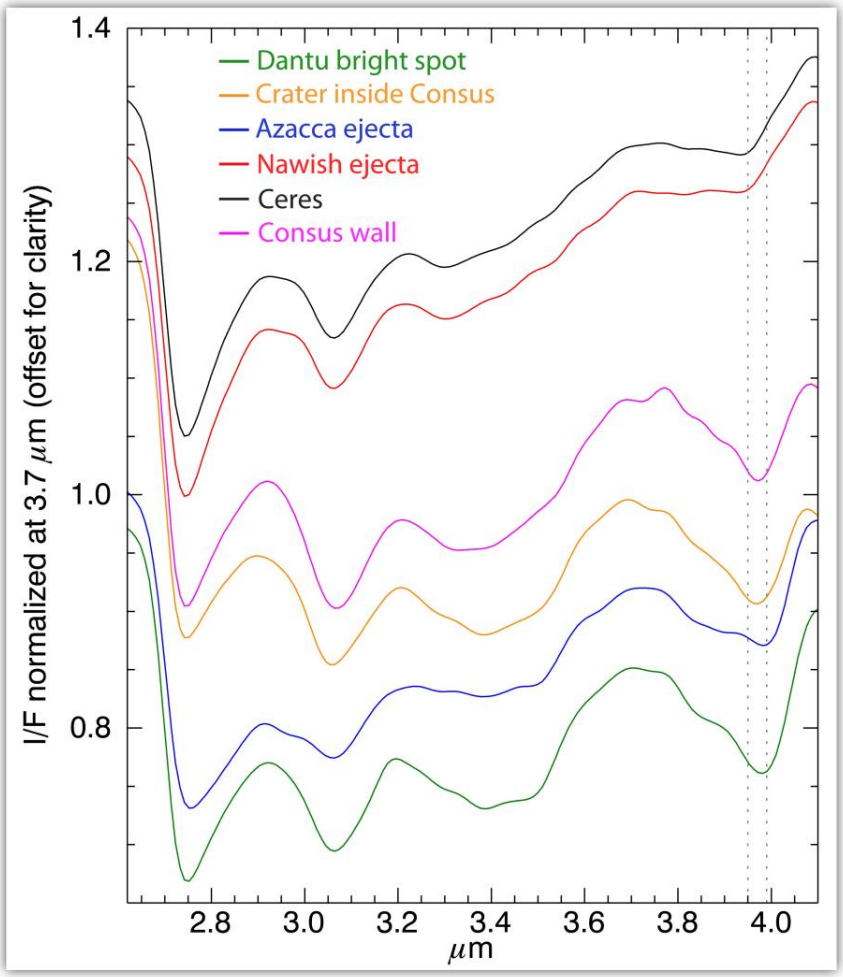

Figure 10. Average spectra of different regions on Ceres surface compared with some areas of interest in Ac-H-8 Nawish quadrangle. The spectra have been normalized to 1 at 3.7 μm. An offset has been applied for clarity. The spectra are an average of 10 pixels. Dotted lines show the shift of the band center at 4 μm, indicating a compositional variation of carbonate species.

4. Description of the quadrangle

Ac-H-8 quadrangle Nawish borders with Ac-H-7 Kerwan quadrangle in the western region (Palomba et al., 2017, this issue), Ac-H-9 Occator in the eastern side (Longobardo et al., 2017, this issue), Ac-H-3 Dantu (Stephan et al., 2017, this issue) and Ac-H-4 Ezinu (Combe et al., 2018, this issue) quadrangles

in the northern part, while Toharu (De Sanctis et al., 2017b, this issue) and Urvara (Longobardo et al., 2017, this issue) quadrangles in the southern side. From a topographical standpoint, Nawish quadrangle can be divided into two distinct regions (Fig. 3): the central and eastern part of the quadrangle is topographically elevated (highlands) and characterized by cratered terrains and the older domain; the western lowlands contain young smooth material and ejecta related to impact craters of Kerwan and Dantu, respectively (~70–150 Ma Kneissl et al., 2016). Ac-H-8 contains some relevant large impact craters, such as Nawish (80 km) and Kumitoga (96 km).

The geological map (Fig. 4) of the quadrangle (Frigeri et al., 2018b) indicates the presence of three major units, cratered terrains (*crt*) which dominate the eastern highlands, smooth material (*sm*), characterizing the western lowlands, and crater material (*c*) typical of the crater ejecta of big impacts. Cratered terrains are the widespread oldest geological unit of Ceres. It is heavily cratered, and the crater counting reveals an age of ~2 Ga (Frigeri et al., 2018b). In *crt*, large craters show degraded rims, while small craters display more prominent rims (Frigeri et al., 2018b). *Sm* resembles the cratered terrains morphology, with a lower amount of craters with a diameter >15 km and a higher albedo. The crater size-frequency counts demonstrate that the *sm* unit is younger than the crt (1 Ga) (Frigeri et al., 2018b). Cm superposes either the older *crt* and the *sm* units. In *c* is present bright ejecta material (e.g. in the ejecta of Azacca crater or in the area around Dantu crater). Other localized geological units, such as lobate material, display bright spots and linear features.

5. Mineralogy of Ac-H-8 Nawish quadrangle

5.1. Colors and topography from FC data

Nawish quadrangle shows variability in terms of spectral parameters, revealing a variation in composition. The RGB color ratio (R: 965 nm/749 nm, G: 555 nm/749 nm, B: 438 nm/749 nm, Fig. 2) shows that most of the surface is reddish, with some localized blue regions in correspondence to bright spots (Palomba et al., 2016), craters' ejecta, such as the Azacca and Dantu ones (Stephan et al., 2017, this issue), and ejecta of unnamed craters in the southern region on Nawish. This color combination can only distinguish two main color units, background (red), and ejecta (blue). We do not observe a correlation between this RGB composite map (Fig. 2) and the topography (Fig. 3). However, a correlation between bluish regions (Fig. 2) and crater material units (Fig. 4) is observed.

5.2. VIR reflectance at 1.2 μm

Albedo map retrieved in the near infrared at 1.2 μm (Fig. 5) shows a dichotomy between the eastern and the western side of the quadrangle. The western side, corresponding with the lowlands, has larger albedo values (mostly in the Dantu ejecta area), while the eastern side, associated with the highlands, and bordering the Occator quadrangle (Longobardo et al., 2017, this issue) appears darker. We observe, as usual, that the older cratered terrains are darker than younger fresher terrains. Albedo can be related both to the grain size and composition. In general on Ceres, an albedo increasing is related with the occurrence of Na-carbonate deposits (e.g. Carrozzo et al., 2018).

5.3 VIR near-infrared spectral slope at 1.163–1.891 μm

The quadrangle is characterized by flat or slightly positive spectral slope values (Fig. 6). In Nawish quadrangle we observe, lower spectral slope regions (bluish material), in correspondence with Dantu, Heneb and Azzacca crater ejecta (Stephan et al., 2017). Redder materials (high spectral slope values)

have been found in an unnamed crater inside the Consus. An isolated radial ejecta, classified as crater ray material (Frigeri et al. 2018b) and located in the center of Nawish quadrangle, shows a slightly bluer slope.

Spectral slope variations are due to space weathering effects (e.g., Riner and Lucey, 2012). In this case, the observed slope variations are more likely related to other causes such as composition, desiccation (Posh et al., 2016), grain size (e.g., Cloutis et al. 2012), or a combination of them. Lower spectral slope values are associated with young terrains, higher spectral slope values are typical of older terrains (e.g. Stephan et al., 2017).

5.4. VIR band depths at 2.7 μm and 3.1 μm

The analysis of the absorption bands at 2.7 and 3.1 μm have been interpreted as due to Mg- and NH_4-rich phyllosilicates, respectively. 2.7 μm band depth values span between 0.18 and 0.20, while the band depth at 3.1 μm ranges between 0.07 and 0.11. These bands do not reveal any band center variation, implying no relevant compositional changes (Ammannito et al., 2016). Conversely, the maps of band depth (Fig. 7, 8) reveal a regional variability. This quadrangle appears depleted in Mg-phyllosilicates in the south-eastern region, where Consus and Azzacca Crater are present, but an enrichment in Mg-phyllosilicates have been observed in correspondence with Nawish and Heneb ejecta, and in the region of Kerwan surroundings. No evidence for a correlation between geological units and this spectral parameter has been found. Conversely, the 3.1 μm band depth, associated to the NH_4-phyllosilicates, shows a dichotomy between the eastern and the western side of the quadrangle. The highlands, characterized by the old cratered terrains unit, are poor in NH_4-phyllosilicates; the lowlands, linked to the smooth material units show a larger amount of ammonia-bearing species. A correlation between

Mg- and NH_4-phyllosilicates is partially observed in this quadrangle. Smooth material unit and cratered material in Azacca and Consus areas show a similar trend in the maps of both the band depths. In the older cratered terrain unit we observe an opposite trend.

5.5. VIR Band center and depth at 4 µm

A weak spectral feature at 4 µm, associated with Mg-carbonates compounds (De Sanctis et al., 2015), is present. Unlike the two bands described in the previous section, the absorption at 4 µm shows a band center variability. It moves toward longer wavelengths indicating a compositional variation (Carrozzo et al., 2018). Generally, the 4 µm bands is centered at 3.95 µm, showing the presence of Mg-carbonates, even if in specific regions, it shifts to 3.99 µm, suggesting the presence of Na-carbonates (De Sanctis et al., 2016, Carrozzo et al. 2018, Fig. 9A). Na-carbonates are generally correlated to the bright albedo material (Fig. 9). These Na-carbonates deposits are mainly located in Dantu and Azacca ejecta, and in Consus crater (see also Stephan et al., this issue; Longobardo et al., this issue; Palomba et al., this issue).

On Ceres, a strong anti-correlation between phyllosilicates and Na-carbonates content is observed (De Sanctis et al., 2015; De Sanctis et al., 2016; Zambon et al., 2017a; Carrozzo et al. 2018). Sodium carbonates rich areas are related with low spectral slope values (bluish material, Stephan et al., 2017), both in the visible and in the infrared range. Not all the bluish materials show sodium carbonate signatures. The bluisher terrains correspond with Azacca and Dantu ejecta, the Heneb crater floor and some medium-size craters (Fig. 6). In Fig. 10 we show some average spectra of Na-carbonates rich regions. Nawish crater ejecta are quite similar to the Ceres average spectrum, while Azacca ejecta,

Consus wall and Dantu bright spot show a considerable spectral variation. These last spectra display a strong band depth at 4 μm.

5. Discussion and conclusions

A thorough analysis of the Ac-H-8 Nawish quadrangle, based on the interpretation of several spectral parameters, indicates a variegated mineralogy. It is characterized by an altitude gap of ~10 km between the two distinct topographical regions: the highlands in the central-eastern part of the quadrangle and corresponding with the older domain, and the western lowlands including two younger domains related to the two impact craters Kerwan and Dantu (~70–150 Ma, see Kneissl et al., 2016). Unlike for most other quadrangles, here we observed a correlation between these two macro-regions and the two main geological units, the young smooth material (~1.1Ga), and the oldest cratered terrains (~2.5Ga), representative of the original crust of the dwarf planet. The oldest areas appear depleted in ammonia-bearing species, unlike the younger smooth material, rich in NH_4-phyllosilicates. We do not observe the same trend for the Mg-phyllosilicates, which are uniformly distributed across the smooth terrains and the crater terrains.

Carbonate deposits are distributed across Ceres, indicating global aqueous alteration of the surface (Carrozzo et al., 2018). In particular, we observe a widespread distribution of (Mg,Ca)-carbonates, although localized areas rich in Na-carbonates have been found in several region of the dwarf planet (Carrozzo et al., 2018), such as in Cerealia and Vinalia faculae in Occator quadrangle (De Sanctis et al., 2016, Longobardo et al., 2017, Raponi et al., 2017), Ahuna Mons (Zambon et al., 2017b), Haulani crater (Tosi et al., 2017; Tosi et al., 2018). In Nawish quadrangle, only a few areas are different from the global distribution of the main spectral parameters, such as at craters inside Consus, Azacca and in

Dantu's ejecta. Generally, these minerals occur with bright material terrains, which are indicative of less processed fresher material. Na-carbonates formed via impact-induced heating in presence of ice and/or are transported to, or near the surface from depth via fractures (De Sanctis et al. 2016; Carrozzo et al., 2018). Conversely to carbonates, the position of band centers in phyllosilicates species does not change (Ammannito et al., 2016), indicating little compositional variations for these compounds. Similarly to other quadrangles also in Nawish, an increase of Na-carbonates correspond with a decrease of phyllosilicates (Carrozzo et al. 2018). Band depth at 3.1 μm seems to correlate with age, but not with the crater size (Stephan et al., 2017, this issue; Frigeri et al., 2018b, this issue). Deeper 3.1 μm band depth has been found in the pristine regions of Dantu (Stephan et al., 2017, this issue) and in the smoothed deposits around Kerwan, suggesting a recent formation. Nevertheless, this correlation is not observed in the Azacca area (~76 Ma (LDM); ~46 Ma (ADM); Scully et al., 2016), where the band depth is very low but the age is comparable with the Dantu one (~111 Ma (LDM), Kneissl et al., 2016). In Azacca ejecta, low band depth corresponds with younger ages, as reported in other quadrangles, such as Toharu and Sinatana (De Sanctis et al., 2017b, this issue). This indicates some difference in the relationship between age and mineralogy.

The 2.7 μm band depth has the similar values for cratered and smoothed material (see Nawish, Heneb and Kerwan areas). The young age of deposits around Kerwan and Dantu (Hiesinger et al., 2016) indicates that a resurfacing in the mineralogy took place in the recent history of the Nawish quadrangle. FC images show bright materials in Dantu ejecta, around Azacca, along the walls of the Consus crater, and in an unnamed crater inside Consus, suggesting the excavation of terrains of different compositions. Alternatively, because Dantu is one of two longitudes on Ceres where water vapor release has been detected, another interpretation is that the bright deposits in the Dantu region could be the result of explosive cryovolcanism (Williams et al., 2016).

In general, Nawish quadrangle represents an area of Ceres where the most ancient crust of Ceres is well preserved and where the mineralogy has similar properties to that of most of the surface of Ceres. However, some local areas show evidence of extensive and global aqueous alteration with some evidence of subsurface compositional differences from place to place that affects the surface. In these areas Na carbonates occur. Their presence in fresh crater-related materials could be consistent with the material mobilized or created by impact induced heating. We are not able to fully discriminate among the possible mechanisms, and likely, the types of Na carbonates and the observed distribution could be the results of a combination of both processes. Although the timing of the mobilization of sodium carbonate remain an open question, their occurrence in younger terrains indicate that the formation/exposure took place in recent history of the Ceres.

Acknowledgments

We thank the Italian Space Agency (ASI). The VIR instrument was funded and coordinated by the ASI and built by Selex ES, with the scientific leadership of the Institute for Space Astrophysics and Planetology, Italian National Institute for Astrophysics, Italy, and is operated by the Institute for Space Astrophysics and Planetology, Rome, Italy. Thanks to the FC team for sharing the camera images.

References

Ammannito E., et al. (2016). Distribution of phyllosilicates on the surface of Ceres, Science, 353(6303).

Beck P., et al. (2011). Goethite as an alternative origin of the 3.1 μm band on dark asteroids, A&A, 526, A85.

Binzel R.P., et al. (2015). Spectral slope variations for OSIRIS-REx target Asteroid (101955) Bennu: Possible evidence for a fine-grained regolith equatorial ridge, Icarus, 256, 22-29.

Carrozzo F.G., et al. (2012). Iron mineralogy of the surface of Mars from the 1 μm band spectral. properties, Journal of Geophysical Research, Volume 117, (E00J17).

Carrozzo F.G., et al. (2016). Artifacts reduction in VIR/Dawn data, Review of Scientific Instruments 87, 124501.

Carrozzo F.G., et al. (2018). Nature, formation and distribution of carbonates on Ceres, Science Advances, vol. 4, no. 3, e1701645.

Clark R.N., et al. (1999). Spectroscopy of Rocks and Minerals, and Principles of Spectroscopy, in Manual of Remote Sensing, Volume 3, Remote Sensing for the Earth Sciences, (A.N. Rencz, ed.) John Wiley and Sons, New York, 3- 58.

Ciarniello M., et al. (2017). Spectrophotometric properties of dwarf planet Ceres from VIR onboard Dawn mission, A&A, 598, A130.

Cloutis E.A., et al. (2012). Spectral reflectance properties of carbonaceous chondrites: 6. CV chondrites, Earth and Space Exploration, Icarus, 221, 1, 328-358

Combe J.-P., et al. (2018). The surface composition of Ceres' Ezinu quadrangle analyzed by the Dawn mission, Icarus, this issue.

Cuzzi J., et al. (2009). Ring Particle Composition and Size Distribution, Saturn from Cassini-Huygens, In: Dougherty M.K., Esposito L.W., Krimigis S.M. (eds) Saturn from Cassini-Huygens. Springer, Dordrecht.

M.C. De Sanctis, et al. (2011). The VIR spectrometer, Space Science Review, 163, 329-369.

De Sanctis M.C., et al. (2015). Ammoniated phyllosilicates with a likely outer Solar System origin on (1) Ceres, Nature, 528, 241-244.

De Sanctis M.C., et al. (2016). Bright carbonate deposits as evidence of aqueous alteration on (1) Ceres, Nature, 536, 54-57.

De Sanctis M.C., et al. (2017a). Localized aliphatic organic material on the surface of Ceres, Science, 355(6326), 719-722.

De Sanctis M.C., et al. (2017b). Ac-H-11 Sintana and Ac-H-12 Toharu quadrangles: Assessing the large and small scale heterogeneities of Ceres' surface, Icarus, this issue.

Filacchione G. and E. Ammannito (2014). Dawn VIR Calibration Document, version 2.4, http://sbn.psi.edu/archive/Dawn/vir/DWNVVIR_I1B/DOCUMENT/VIR_CALIBRATION/VIR_CALIBRATION_V2_4.PDF.

Filacchione G., et al. (2012). Saturn's icy satellites and rings investigated by Cassini– VIMS: III – radial compositional variability, Icarus, 320 (2012), pp. 1064-1096.

Frigeri A., et al. (2018a). The spectral parameter maps of Ceres from NASA/DAWN VIR data, Icarus, this issue.

Frigeri A., et al. (2018b), The Geology of the Nawish Quadrangle of Ceres, Icarus, submitted.

Greeley R. and M. Batson, Planetary mapping (Cambridge University Press, 296 p. : ill., maps ; 29 cm, 1990).

Hapke B. (2012). Theory of reflectance and Emittance Spectroscopy (Cambridge Univ. Press).

Hiesinger H., et al. (2016). Cratering on Ceres: implications for its crust and evolution, Science, 353, 6303, aaf4759.

Johnson T.V. and F. Fanale (1973). Optical properti3s of carbonaceous chondrites and their relationship to asteroids, J. Geophys. Res. 78, 8507-8518.

King T.V., et al. (1992).Evidence for ammonium-bearing minerals on Ceres, Science, 255, 1551-3.

Kneissl T., et al. (2016). Geologic Mapping of the Ac-H-3 Dantu Quadrangle of Ceres from NASA's Dawn Mission, 47th LPSC, abstract #1967.

Larson H.P., et al.(1979). Remote spectroscopic identification of carbonaceous chondrite mineralogies Applications to Ceres and Pallas. Icarus 39, 257–271.

Lebofsky L.A. (1978). Asteroid 1 Ceres: evidence for water of hydration, Mon. Not. R. astr. Soc., 182, 17-21.

Lebofsky L.A., et al. (1981).The 1.7- to 4.2-micron spectrum of asteroid 1 Ceres - Evidence for structural water in clay minerals, Icarus, 48, 453-459.

Longobardo A., et al. (2017). Mineralogy of the Occator quadrangle, Icarus, in press.

McCord T.B. and J. C. Castillo-Rogez (2018). Ceres' internal evolution: The view after Dawn, MAPS, in press.

McSween H.Y., et al. (2017). Carbonaceous chondrites as analogs for the composition and alteration of Ceres, Meteoritics & Planetary Science.

Milliken R.E., and A.S. Rivkin, (2009). Brucite and carbonate assemblages from altered olivine-rich materials on Ceres, Nature Geoscience, 2, 258-261.

Morbidelli A., et al. (2009). Asteroids were born big, Icarus 204, 558-573.

Palomba E., et al. (2017). Mineralogical mapping of the Kerwan quadrangle on Ceres Icarus, in press.

Pelkey S.M., et al. (2007). CRISM multispectral summary products: parameterizing mineral diversity on Mars from reflectance, J. Geophys. Res., 112, E08S14.

Perna D., et al. (2015). Short-term variability on the surface of (1) Ceres, A&A, 575, L1.

Poch O., et al. (2016). Sublimation of water ice mixed with silicates and tholins: Evolution of surface texture and reflectance spectra, with implications for comets, Icarus, 267, 154–173.

Preusker F., et al. (2016). Dawn at Ceres - Shape Model and Rotational State, 46th LPSC, abstract #1954.

Raponi A.,et al. (2017). Mineralogical mapping of Coniraya quadrangle of the dwarf planet Ceres, Icarus, this issue.

Riner M.A. and P.G. Lucey 2012). Spectral effects of space weathering on Mercury: The Role of Composition and Environment, Geophysical Research Letters, 39, 12,

Rivkin A.S., et al. (2006). The surface composition of Ceres: discovery of carbonates and iron-rich clays, Icarus, 185(2), 563-56.

Roatsch T., et al. (2016). High-resolution Ceres high altitude mapping or- bit atlas derived from Dawn framing camera images, Icarus 129, 103–107.

Russell C.T. and C.A. Raymond (2011). The Dawn Mission to Vesta and Ceres, Space Sci Rev, 163, issue 1-4, 3-23.

Russell C.T., et al. (2016). Dawn arrives at Ceres: Exploration of a small, volatile-rich world, Science, Volume 353, Issue 6303, pp. 1008-1010.

Schröder S.E., et al. (2013). In-flight calibration of the Dawn Framing Camera, Icarus, 226, 2, 1304-1317.

Scully J.E.C., et al. (2016).Geological Mapping of the Ac-H-4 Ezinu Quadrangle of Ceres from NASA's Dawn Mission, 47th LPSC, abstract #1627.

Sierks H., et al. (2011). The Dawn Framing Camera.Space Science Reviews, 163, 263-327.

Stephan K., et al. (2017). Spectral Investigation of Quadrangle Ac-H-3 of the Dwarf Planet Ceres - The Region of Impact Crater Dantu, Icarus, this issue.

E.F. Tedesco, et al. (1983). Worldwide photometry and lightcurve observations of 1 Ceres during the 1975–1976 apparition. Icarus 54, 23–29.

Tosi F., et al. (2017). Mineralogical analysis of the Ac-H-6 Haulani quadrangle of the dwarf planet Ceres, Icarus. This issue.

Tosi F., et al. (2018). Mineralogy and temperature of crater Haulani on Ceres, Meteoritcs & Planetary Science, in press.

Vernazza P., et al.(2005). Analysis of near-IR spectra of 1 Cres and Vesta, targets of the Dawn mission, A&A, 436, 1113-1121.

Zambon F., et al. (2017a). Spectral analysis of Ahuna Mons from Dawn mission's visible-infrared spectrometer. Geophys. Res. Lett. 44, 97–104.

Zambon F., et al. (2017b). Mineralogical analysis of quadrangle Ac-H-10 Rongo on the dwarf planet Ceres, Icarus, this issue.

Williams D.A., et al. (2016). Geologicic mapping of the Ac-H-7 Kerwan quadrangle of Ceres from Nasa's Dawn mission, 47th LPSC, abstract #1522.